

Accepted Manuscript

Research papers

Regional flood-frequency reconstruction for Kullu district, Western Indian Himalayas

J.A. Ballesteros Cánovas, D. Trappmann, M. Shekhar, A. Bhattacharyya, M. Stoffel

PII: S0022-1694(16)30857-5

DOI: <http://dx.doi.org/10.1016/j.jhydrol.2016.12.059>

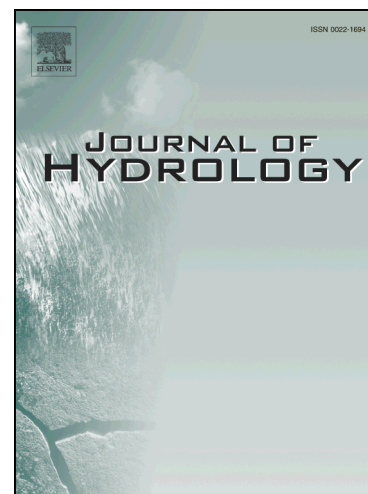
Reference: HYDROL 21738

To appear in: *Journal of Hydrology*

Received Date: 13 October 2016

Revised Date: 26 December 2016

Accepted Date: 31 December 2016



Please cite this article as: Ballesteros Cánovas, J.A., Trappmann, D., Shekhar, M., Bhattacharyya, A., Stoffel, M., Regional flood-frequency reconstruction for Kullu district, Western Indian Himalayas, *Journal of Hydrology* (2016), doi: <http://dx.doi.org/10.1016/j.jhydrol.2016.12.059>

This is a PDF file of an unedited manuscript that has been accepted for publication. As a service to our customers we are providing this early version of the manuscript. The manuscript will undergo copyediting, typesetting, and review of the resulting proof before it is published in its final form. Please note that during the production process errors may be discovered which could affect the content, and all legal disclaimers that apply to the journal pertain.

10 **Abstract**

11 Floods are a major threat in many valleys of the Indian Himalayan Region (IHR). Yet, the lack
12 of reliable data on past events renders the implementation of appropriate adaptation policies a
13 difficult task, and therefore also hampers the mitigation of future disasters. In an attempt to
14 overcome these shortcomings, we combine reconstructed paleoflood events based on tree-ring
15 analyses with existing systematic records, so as to derive a regional flood frequency. Analysis
16 was realized with tree-ring records and through the dating of growth disturbances in riparian
17 trees of major rivers in Kullu district (Himachal Pradesh, Indian Himalayas). To this end, we
18 combined field-based observations, tree-ring analyses, hydraulic modelling and statistical
19 approaches. Results suggest that the occurrence of floods in Kullu district is recurrent, with a
20 marked seasonality and a cyclic natural variability in flood frequency at multi-decadal scales, as
21 well as distinct spatial representativeness. The inclusion of peak discharge data of past,
22 previously ungauged, flood events derived from tree-ring records has a significant and positive
23 impact on the flood frequency assessment. Flood hazards and associated risks have been clearly
24 underestimated in the region and based on the systematic records alone. We also demonstrate
25 that a regional flood frequency approach is suitable to optimize the information gathered from
26 tree rings and that flood frequency can thus be analyzed for larger regions. The approach used in
27 this paper can be implemented in the other, poorly gauged region and thus contribute to climate
28 change adaptation policies in undocumented environments such as the Indian Himalayan Region.

29 **Keywords:** past food, flood frequency, hazard, tree rings, Kullu district, Indian Himalayas.

30 **1 Introduction**

31 Extreme floods represent the most frequent and widespread type of natural disaster in the Indian
32 Himalayan Region (IHR) (Gardner, 2002; Gardner and Saczuk, 2004). Almost each year, flood
33 disasters occur in its headwater catchments and thereby cause substantial economic losses and
34 high death tolls in downstream valleys, thereby disrupting infrastructures and stressing the status
35 quo of local communities. Recently, the occurrence of a series of very dramatic disasters has
36 underlined the high vulnerability of the region. In August 2010, a heavy downpour and
37 subsequent flash floods have killed more than 250 persons in Ladakh and damaged 71 villages
38 (Hobley et al., 2012). The early onset of unusually intense monsoon rainfalls in June 2013
39 caused more than 6000 casualties at Kedarnath (Uttarakhand) (Allen et al., in press). The most
40 recent event on record occurred in Jammu and Kashmir when floods flooded major riverine cities
41 (such as Srinagar) in September 2014 and March 2015 (Ballesteros-Cánovas et al., 2016),
42 causing numerous fatalities and substantial economic losses.

43 Several studies have argued that ongoing climate change (GCC) was at the origin and the
44 causative reason for the clustering of recent flood disasters, and therefore suggested an increase
45 of situations favoring flood occurrences and exacerbation of flood severity over the next decades
46 (Hirabayashi et al., 2013). Most often, changes in monsoon rainfall over India were held
47 responsible for the recent peak in flood disasters and for those that might come in the future
48 (Attri and Tyagi, 2010; Mathison et al., 2013; Turner, 2013). Besides, some authors have also
49 pointed to the galloping economic development in the IHR and to the lack of preparedness and
50 planning in most flood-prone areas, and have identified these socio-economic changes as the
51 major and most significant amplifiers of flood impact (i.e. Gardner, 2002). While it is possible
52 that the current flood situation could in fact deteriorate further over the next decades and as a

53 result of GCC, it is also the extensive use of floodplains and the generalized lack of proper flood
54 hazard zonation which renders the situation in the region critical, even in the absence of GCC.

55 The implementation of suitable adaptation policies, as part of a sustainable development process,
56 requires therefore better knowledge of critical processes and a proper identification of the areas
57 affected by floods (National Disaster Management Policy, 2009). Recently, the first Disaster
58 Management Regulation has been implemented at the national level by the Government of India
59 (i.e. Disaster Management Act, 2005), but the implementation of disaster preparedness strategies
60 in the IHR has remained a very challenging process. As commonly recognized in the Hyogo
61 Framework (UN, 2005), this challenge is very much related to the generalized lack of long-term
62 flow records and the documentation of historical flood disasters, which is not only a problem in
63 the IHR, but in most (mountain) regions of the World. For as long as such data are missing,
64 rational flood hazard assessment and risk awareness of local citizens and authorities will,
65 however, remain rather constrained.

66 In high mountain regions, lacking baseline data of past extreme events is a common and
67 widespread problem (Ballesteros-Canovas et al., 2015; Bodoque et al., 2015; Stoffel et al., 2010).
68 Although not readily available for administration, policy, and decision makers in the form of
69 reports or statistics on flood quantiles, data on past disasters and the gauging of ungauged
70 catchments would indeed be possible in many mountain regions of the world, including the IHR.
71 In fact, field-based geomorphic, botanical, or historical records are often readily available in
72 these regions and can be used to describe and document the hydrodynamics of past flood in
73 ungauged catchments with up to seasonal precision and over multi-centennial timescale (Baker,
74 2008). More specifically, tree rings have been used repeatedly in mountain environments to
75 document past disasters (Stoffel et al., 2010), and have been demonstrated to have several

76 advantages over other approaches when it comes to flood reconstructions in mountain streams
77 (Ballesteros-Canovas et al., 2015a). The approach is based on the concept that trees affected by
78 hydrogeomorphic processes will conserve information on the event in their growth-ring records
79 (Shroder, 1978; Stoffel and Corona, 2014; Stoffel and Wilford, 2012), and that the analysis of
80 tree-ring series of riparian vegetation can thus be used to infer the frequency and magnitude of
81 individual floods (Ballesteros-Canovas et al., 2015a). The applicability of tree-ring records for
82 Disaster Risk Reduction (DRR) has been tested in several mountain streams worldwide with the
83 aim to document past flood activity and to decipher flood-climate linkages at the catchment
84 (Ballesteros-Cánovas et al., 2015; Ballesteros et al., 2011; Ballesteros Cánovas et al., 2011;
85 Ballesteros et al., 2010ab; Corriell, 2002; McCord, 1990; Ruiz-Villanueva et al., 2013; St.
86 George and Nielsen, 2003; Therrell and Bialecki, 2015; Yanosky and Jarret, 2002; Zielonka et
87 al., 2008) or regional (e.g., Ballesteros-Cánovas et al., 2015b, c; Rodriguez-Morata et al., 2016;
88 Šilhán, 2015) scales.

89 In analogy to geological and historical flood records (Gaál et al., 2010; Gaume et al., 2010;
90 O'Connell, 2005; O'Connor et al., 1994), tree-ring based flood reconstructions can contribute to
91 important changes in the flood frequency distributions and thus can help to improve existing
92 flood records and to reduce uncertainties related to flood processes (in terms of both frequency
93 and magnitude) in a substantial manner (Ballesteros-Cánovas et al., 2013; Ballesteros-Cánovas
94 et al., 2015c). Information derived from tree rings has also been used to analyze the non-
95 stationary behavior of flood-prone catchments and to address its implications in terms of flood
96 hazard zonation (Brooks and St George, 2015), with major impacts on future flood risk
97 assessments. However, all of these experiences have focused at the catchment scale, and have, at
98 best, assessed hazards in the same sub-system. Yet, the potential of an incorporation of tree-ring-

99 based peak flood reconstruction into flood frequency assessments at the regional scale has
100 remained unexplored.

101 Accordingly, this paper aims at dating past flood activity in Kullu district (Himachal Pradesh,
102 Indian Himalayas) at the regional scale and at virtually extending the network of existing flow
103 gauge network across the region. We combine flood reconstructions from sub-catchments of the
104 Beas river for a regional flood frequency assessment comprising the entire Kullu district. To this
105 end, tree-ring analyses have been combined with field-based recognition, hydraulic approaches,
106 and Bayesian statistical procedures. In this paper, we present a regional flood frequency
107 estimation for the Kullu region and compare results with data derived from instrumental records
108 in terms of flood quantiles and uncertainties in the estimates. Our results can be used as a basis
109 for the definition of policies aimed at climate change adaptation to natural disaster in the study
110 region or at the scale of larger regions within the IHR.

111 **2 Physical setting: Kullu District, Himachal Pradesh, India**

112 The rivers chosen for the regional flood reconstruction are located in Kullu district ($\sim 5.5 \times 10^3$
113 km^2), in the state of Himachal Pradesh, where population is in the order of $>4 \times 10^5$. The study
114 region is located close to the Great Himalayan National Park at around $\sim 32^\circ \text{N}$ and $77^\circ 2' \text{E}$ (Fig.
115 1) and also includes the tourist mecca of Manali. This part of the IHR is characterized by a main
116 valley running in north-south direction, formed by the Beas River; as well as by a series of
117 tributary valleys shaped, among others, by the action of the Parvati, Sainj, and Thirtan Rivers.
118 The river valleys are generally characterized by wide bottom floodplains occupying large parts
119 of the U-shaped valley floors. The valley floors also are hotspots of population and
120 transportation. The tributary rivers are characterized by narrow side valleys, forcing inhabitants

121 to live on the steeper slopes or on the limited, yet often flood-prone, flatter surfaces in the valley
122 bottoms.

123 Forest cover represents more than 35% in the study region and comprises both broadleaved and
124 conifer taxa, with the latter being more prominent at higher elevations. Forests of *Alnus nitida*
125 associated with *Ulmus* sp. and *Populus* sp. are common in new floodplains whereas *Cedrus*
126 *deodara* and *Pinus wallichina* are prevailing on older flood deposits. In terms of climate, the area
127 is influenced by both westerlies and the south-western influence of the monsoon. Climate in the
128 region ranges from alpine, cold temperate, warm temperate to subtropical, as do forest types as
129 per the classification of Champion and Seth (1968). At the level of the settlement of Kullu,
130 average air temperatures range from -4° to 20°C in winter and up to 35°C in summer. During the
131 monsoon period, monthly rainfall typically exceeds 150 mm, which is beneficial for local
132 agriculture/horticulture representing the single-most important sector in Kullu district (74% of
133 the GDP). In recent years, however, tourism (both national and international) has gained
134 momentum and increased significantly in the area (Sah and Mazari, 2007).

135 Existing hydro-meteorological records at Kullu district consist of two rain gauge stations and
136 twelve flow gauge stations. However, flow gauge records are highly fragmented, and multi-
137 decadal records are exclusively available for Beas River; this series exists since the late 1960s
138 (see Supplementary Information for details)

139 **3 Material and Methods**

140 3.1 Tree-ring based flood dating

141 This study started with a field survey and aerial picture recognition to detect the most suitable
142 river reaches for tree-ring reconstructions. Analyses focused on six river reaches in the Upper
143 Beas, Paravati, Thiertan, and Sainj river catchments and included the collection of eye-witness
144 data (i.e., pictures and videos) on recent floods events as well as interviews with the local
145 population, forest, and village authorities. This initial contact was essential for the engagement of
146 the local population in the study and greatly facilitated further analyses and interpretations. At
147 each of the river reaches assessed in this study, we applied classical tree-ring sampling of trees
148 affected by floods and recorded their position along the channel and in the floodplain
149 (Ballesteros-Canovas et al., 2015a). In addition, we also included samples taken from trees
150 growing in undisturbed forest stands so as to build reference chronologies representing local, yet
151 undisturbed growth conditions. Increment borers and hand saws were used to obtain increment
152 cores and wedges from disturbed trees. We preferentially sampled trees with visible abrasion
153 scars induced by debris transported during past floods (Ballesteros et al., 2011; Ballesteros
154 Cánovas et al., 2011), as these are considered the most reliable signal for flood reconstructions
155 (Ballesteros-Canovas et al., 2015a; St. George, 2010). To detect hidden scars, older trees
156 growing close to the channel in exposed locations with respect to the flow were sampled as well,
157 as hidden scars can often be dated indirectly (Arbellay et al., 2010; 2012a,b; Ballesteros et al.,
158 2010ab; Schneuwly et al., 2009; Stoffel and Perret, 2006). Additional information, such as the
159 geographical location and graphical information of the tree and the channel reach as well as river
160 cross-sectional topography and the maximum height of the scars (i.e. paleostage indicator, PSI),
161 were recorded as well and by using a GPS, camera, laser distometer (TruePulse 3600B,
162 precision: 30 cm), tape measure, and clinometer. A total of 256 increment cores and 27 cross-
163 sections and wedges were sampled from 177 disturbed *Pinus wallichina*, *Alnus nitida*, *Ulmus* sp.,

164 and *Populus* sp. trees at six different study reaches. In addition, we sampled 35 undisturbed
 165 samples of *Abies pindrow* and 55 cores from *Cedrus deodara* to build two reference
 166 chronologies and to separate climate signals from flood impacts in the affected trees.

167 In the lab, we sanded all samples and counted their rings before the growth series were cross-
 168 dated using skeleton plots. During this step, we used extremely narrow rings from two reference
 169 chronologies as benchmark years for the cross-dating. Using a stereomicroscope, we then
 170 identified growth disturbances (GD) related to floods, namely scars and injuries, callus tissue and
 171 reaction wood (Stoffel and Corona, 2014). Definition of past flood events was based on the
 172 weighted index value (W_{it} ; see Kogelnig-Mayer et al., 2011), which considers the number,
 173 intensity, and typology of GDs within each tree-ring series and the total number of trees
 174 available for the reconstruction at any moment of the past (thus taking account of reduced
 175 sample availability as one goes farther back in time). We only accepted flood-event in those
 176 years for which we observed GDs in more than two trees and for which the W_{it} was >0.8
 177 (Ballesteros-Cánovas et al., 2014).

178 In a next analytical step, we combined flood occurrence data from all catchments, i.e. the
 179 reconstructed (tree-ring based) floods and the flow records of existing gauge stations, to derive a
 180 regional flood activity index (RFAI) as follows:

$$181 \quad RFAI = \frac{\sum_t^i (F_{tree} + F_{gauge})}{\sum_1^i Rc}$$

182 where F_{tree} represents dated floods in year t in the four catchment (i.e. Beas, Parvati, Sainj, and
 183 Thiernan); F_{gauge} indicates the number of measured flows ($>90^{th}$ of flow record) at the gauge
 184 station for each catchment in year t ; and where Rc represents the number of catchments reacting

185 in year t . The index we use is similar to the one used for snow avalanche reconstructions
186 (Germain et al., 2009), and aims at limiting possible bias in the composite analysis associated to
187 dissimilar sample depths and at reflecting a homogeneous regional flood activity in the study
188 region.

189 3.2 Peak discharge reconstruction

190 Due to the lack of detailed topographic information (e.g., high-resolution Digital Elevation
191 Model or LiDAR data), which are needed to run hydraulic models (Ballesteros Cánovas et al.,
192 2011), we used Manning's equation to transform the height of dated scars on trees (Fig. 2) into
193 peak flow discharge at each of the cross-sections surveyed in the field (Jarrett and England,
194 2002). At each surveyed cross-section, we measured the slope of the main channel and the
195 maximum scar height at each position where a tree was sampled. We are well aware that this
196 procedure is strongly biased by the initial hydraulic assumption (Jarret, 1985). as Manning's
197 equation assumes uniform flow, in which the water-surface and energy gradient are parallel to
198 the channel slope; and the area and hydraulic radius remain constant along the reach river (Jarret,
199 1985). Moreover, we are also aware of the uncertainties related to the calibration of roughness
200 parameters, which can stem from the mixture of water and sediment in the rivers analyzed
201 (Bodoque et al., 2015), as well as to the assumed invariability of channel geometry (Ballesteros
202 et al., 2011). For this reason, analysis has been restricted to uniform river reaches for which
203 bedrock or stable floodplain situations should have prevailed over longer periods of the past, so
204 as to avoid uncertainties in peak discharge reconstruction due to vertical (and horizontal)
205 changes in channel topography. Thus, uncertainties in peak discharge have been incorporated by
206 varying the specific roughness as a uniform distribution ($\pm 25\%$) with respect to the initial set of
207 values gathered in the field and in line with the typology of river reaches as provided by Chow

208 (1964) (i.e. $n=0.06$). The resolution of the equation and estimated parameters are provided in the
209 Supplementary Information.

210 **Figure 2**

211 3.3 Regional flood-frequency analysis

212 Reconstructed peak discharge values and related uncertainty were incorporated as a range of
213 values into the systematic record of the flood frequency analysis. We applied a regional flood
214 frequency analysis approach based on Bayesian Markov Monte Carlo Chain algorithms (Gaume
215 et al., 2010). In addition, a Generalized Extreme Value distribution (GEV) has been used to
216 derive flood quantiles. Homogeneity of the existing systematic flow series has then been tested
217 using the Hosking and Wallis (1987) algorithm, which compares the variation between-site in
218 samples L_{cv} (coefficient of L-variation) for the analyzed sites. The regional flood frequency
219 analysis therefore allows inclusion of flood quantile estimations at different catchment locations
220 by flow-index regionalization. This approach is based on the distribution of a flow discharge
221 from different catchments of a homogenous region. Analysis was performed by using the R
222 package nsRFA (Viglione et al., 2014). The robustness of this method has been tested previously
223 in other hydrological contexts (Gaume et al., 2010). A depth theoretical and practical description
224 of the procedure followed in this paper can be found in Gaál et al. (2010). Finally, we compared
225 the impact which the addition of tree-ring based records to systematic series has on flood
226 quantiles and uncertainties at each of the study catchments.

227 4 Results

228 4.1 Temporal flood reconstruction at Kullu district

229 Dating of the tree-ring sequences from both the increment cores and (partial) cross-sections of
230 trees affected by floods allowed identification of 33 past floods in Kullu district since the early
231 20th century. Most of the dated floods were restricted to the period 1960-2014, this is because
232 older trees were not readily available in the floodplains, either as a result of their frequent
233 removal by floods, or due to human pressure and use. Based on the ten available flow gauge
234 records, we identify 42 years during which flow exceeded the 90th percentile for the length of the
235 record. Figures 3 and 4 show the temporal reconstruction of floods in the different catchments
236 analyzed at Kullu district. By considering only those floods which were either recorded by one of
237 the flow gauge stations or reconstructed in the tree-ring records in one of the six river reaches in
238 the four catchments analyzed, we identify at least 56 flood incidents since 1965, defining an
239 average occurrence rate of floods of almost 1.1 events year⁻¹.

240 Sainj river exhibits the largest number of reconstructed floods based on tree-ring records, with 11
241 ungauged events since 1977 (sample size = 51 trees). Years with ample evidence of floods
242 include 1977, 1988, 1995, 1997, 2001, 2003, 2005, 2006, 2009, 2010, and 2011. By contrast, the
243 smallest number of reconstructed events was found at Beas River, with 5 reconstructed flood
244 events during the last decade (sample size = 30 trees: 2005, 2006, 2010, 2011, and 2012). The
245 limited amount of evidence found at this catchment is related to the young age of vegetation
246 which is in turn also reflects high flood activity in the fluvial domain. In the Thiertan river, 9
247 ungauged flood events have been reconstructed over the course of the 20th century and based on
248 evidence found in 53 trees, namely in 1910, 1919, 1971, 1974, 1980, 2002, 2005, 2008, and
249 2010. At Parvati river, we reconstructed 8 floods based on evidence found in 43 disturbed trees,
250 namely in 1993, 2003, 2005, 2008, 2010, 2011, 2013, and 2014.

251 The spatial inter-catchment comparison of floods reveals that events at Kullu district operate at
252 both regional and catchment-specific scales, and point to the presence of two major local-to-
253 larger scale triggering mechanisms, i.e. high-intensity, but short-lived rainfalls (i.e. mostly
254 cloudbursts) and longer duration, but less intense rainfall events (i.e. monsoon rains). A total of
255 56% of all flood years can be observed in more than two catchments, and in 15% of the cases,
256 flood signals are discernible in more than four catchments. By contrast, and for the remaining
257 44% of flood years, reactions were exclusively found in one specific catchment. The RFAI index
258 also suggests dissimilar flood activity over the past few decades, with distinct phases which were
259 rich or poor in floods. Periods with high activity can be found between 1977-1981, 1988-1995,
260 and 2003-2014, whereas low flood activity is observed between 1981-1987 and 1996-2001.

261 Figure 3

262 Figure 4

263 Table 1

264 4.2 Ungauged floods and regional flood frequency analysis

265 A total of eight intense, yet ungauged flood events have been reconstructed at the river reaches
266 of Kullu district (Table 2). At Sainj valley, trees growing in the river reach located next to the
267 settlement of Ropa (drainage area of ca. 470 km²) showed evidence of 7 major floods during
268 which reconstructed peak discharges ranged from 233 to 824 m³/s. The ungauged events in this
269 catchment took place in 1978 (655 ± 169 m³/s), 1997 (244 ± 88 m³/s), 2003 (494 ± 127 m³/s),
270 2005 (719 ± 185 m³/s), 2006 (639 ± 164 m³/s), 2009 (191 ± 49 m³/s), and 2011 (181 ± 46 m³/s).
271 In the Thiertan valley, we reconstructed a major flood in 2005 with a reconstructed peak

272 discharge of $1869 \pm 482 \text{ m}^3/\text{s}$. All measurements at each of the cross sections are provided in the
273 Supplementary Information.

274 The Hosking and Wallis test was applied on ten flow gauge records covering the period 1964 to
275 2010 and contributing catchment areas ranging from 22 and 3836 km^2 ; it yielded a $H1$ value of -
276 0.05, therefore indicating that the dataset used in this study can be assumed homogeneous for as
277 long as $H1 \leq 1$ (see Supplementary Information). Figure 5 provides an example of differences in
278 flood quartiles, including uncertainties at the 90% interval confidence level, between the regional
279 flood frequency obtained in this study and extrapolated estimates based on the flow gauge data
280 from the Telara dam in Sainj valley alone. Quantitative comparison between the flood frequency
281 data using only the existing flow gauge records and the regional approach combining tree-ring
282 and flow gauge records exhibits major differences for e.g., the 100-year flood quartiles with
283 average differences between the series of up to $+76 \pm 81\%$. In a similar way, mean differences in
284 the uncertainties are in the order of $-41 \pm 59\%$ (Table 3). We therefore demonstrate that flood
285 hazards in Kullu district have been systematically underestimated so far and by using exclusively
286 the available set of fairly short and incomplete systematic records.

287 Figure 5

288 Table 2

289 Table 3

290 **5 Discussion**

291 5.1 Flood occurrences at Kullu district

292 In this paper, we have shown how tree-ring records can be used to inform authorities and the
293 population about the frequency and magnitude of flood events in a selection of poorly gauged
294 catchments of the IHR. In addition, we have provided examples of how regional flood frequency
295 information can be obtained. Based on the analysis of 177 disturbed trees from the four main
296 river catchments of Kullu district, we have added 33 ungauged floods since 1910 to the archival
297 record. In combination with the short (and sometimes incomplete) flow records gathered from
298 ten gauge stations, we also analyzed spatio-temporal patterns of floods at Kullu district and
299 provide insights into cyclic flood variability and high spatial representativeness of the records
300 provided here. Besides, the reconstructed peak discharges of eight intense floods have been
301 merged with data from instrumental flow series to produce a new, regional flood frequency
302 assessment. We therefore probed whether the inclusion of extreme ungauged flood events into
303 the regional flood frequency would indeed result in substantial changes of flood quartiles and the
304 related range of uncertainty.

305 Our results provide clear evidence that flood incidents at Kullu district occurred more than once
306 per year since at least the 1960s ($1.1 \text{ event year}^{-1}$), i.e. for the time for which we have reliable
307 data. Our approach considered both tree-ring and instrumental flow records (for which we only
308 considered exceedances of the 90th percentile). In addition, we realize that the reliability of the
309 flood reconstruction is well-supported by historical and flow gauge records from the valleys, at
310 least for those events which occurred during the last four decades (i.e., 1971, 1978, 1988, 1989,
311 1995, 2005, and 2013). These events have been recorded in the EM-DAT (www.emdat.be) and
312 DFO (www.dartmouth.edu) databases and are well presented in our reconstructions. Our results
313 also match with data from earlier work (Parthasarathy et al., 1987), where the occurrence of
314 several droughts and floods have been reported based on substantial departures from normal

315 rainfall conditions over the period 1871-1984. In this study, the 1970s are shown as a decade
316 with intense flood conditions, which also coincides with a reported shift in monsoon behavior
317 (Terray and Dominiak, 2005; Yim et al., 2014). At the same time, however, the tree-ring based
318 approach also points to the occurrence of twenty additional flood events which have not been
319 documented for Kullu district so far. This outcome suggests that historical datasets clearly
320 underrepresent flood activity in the study region – as is the case also in other mountain regions of
321 the world. Consequently, relying exclusively on systematic datasets will represent a limitation,
322 with potentially major impacts on Disaster Risk Management (DRM) and on the design of
323 mitigation and adaptation plans.

324 The regional flood index weights the impact of the dissimilar availability of gauge station data
325 and/or tree rings to record floods and provides a homogeneous dataset of flood occurrence in the
326 four catchments investigated. Even though the nature of available data sources, heterogeneous
327 over time, does not allow deriving robust long-term trends from our flood chronologies, the
328 index suggests frequent flood occurrences in Kullu district since the late 1960s, however with
329 marked and cyclic flood variability over time. In fact, several studies postulate a causal linkage
330 between monsoon variability and the El Niño Southern Oscillation (ENSO; Kripalani and
331 Kulkarni, 1997; Rajeevan et al., 2008; Ranatunge et al., 2003). However, unlike other parts of
332 the globe, on the Indian subcontinent, ENSO can so far only be held responsible for its influence
333 on monsoon rainfall patterns and to the extent of its year-to-year variability and linkage with
334 occurrences. A positive trend in flood occurrences was recognized by DST (2012) at multi-
335 decadal timescales for Himachal Pradesh, but are partially in disagreement with monsoon rainfall
336 observations, for which trends have been shown to decrease recently (Kumar et al., 2005).

337 Moreover, Chase et al. (2003) and Duan et al. (2006) suggested that monsoon activity would
338 have decreased over the Himalayas since the mid-20th century.

339 We explain this apparent mismatch between monsoon rainfall and flood trends by the dissimilar
340 triggering mechanisms involved in the occurrence of floods at Kullu district. Indeed, spatial
341 analysis of past flood occurrences at Kullu district suggests that an important number of past
342 events would have been limited to individual catchments. The lack of widespread flooding
343 response would in fact point to localized cloudbursts as a trigger of extreme floods, and less so
344 (but also) to monsoon rainfalls, which is consistent with other studies realized in the state of
345 Himachal Pradesh (Sah and Mazari, 1998, 2007). In addition, and in the context of the recent
346 Kedarnath disaster in Uttarakhand, Allen et al., (in press) suggested that rather localized, extreme
347 rainfall events, in combination with other hydro-geomorphic processes (such as the temporary
348 formation and subsequent failure of landslide dams; Ruiz-Villanueva et al., 2016) can indeed
349 trigger larger and more severe events in smaller-scale catchments than would monsoon rainfalls
350 (alone) in the same environments. The fact that only five flood events occurred in all four
351 catchments during the same year points to very extreme and localized rainfall precipitation event
352 as the major, and presumably the most important, triggering mechanism of floods at Kullu
353 district. Yet, the annual-to-seasonal resolution of tree-ring proxies does only allow dating of
354 events to the month at best (e.g., Stoffel, 2008; Stoffel and Wilford, 2012), but does not allow
355 confirmation of a simultaneous (i.e. daily resolution) occurrence of floods in the different
356 catchments. In fact, the highly localized nature of extreme rainfall events in headwater catchment
357 of the IHR is such that a monitoring of these events is difficult, even today, due to the
358 generalized lack of rain-gauge stations in the region or the impossibility to access existing time
359 series of rainfall. Despite the generalized absence of evidence, which would be needed for an

360 attribution of reconstructed floods to specific rainfall events, the high frequency of flood events
361 in the headwater catchments is in line with the rising trend observed in the frequency of heavy
362 rainfall events in the region since the 1950s (Goswami and Xavier, 2005).

363 5.2 Impact of tree-ring based flood reconstruction on regional flood frequency 364 assessments

365 The inclusion of peak discharge reconstructions into the regional flood frequency analyses has
366 important consequences on flood quartiles. If one compares the 100-year quartile of the
367 systematic record with the series including both systematic and reconstructed peak discharge
368 values, substantial changes become apparent in both expected discharge values and in terms of a
369 reduction of uncertainties. Similar changes in flood quartiles have been obtained elsewhere and
370 by comparing systematic data with conventional historical records (Gaál et al., 2010; Gaume et
371 al., 2010), sediment-based reconstruction (Benito et al., 2003; Kjeldsen et al., 2014; Stedinger,
372 2001) or tree-ring-based reconstructions (Ballesteros-Cánovas et al., 2013; Ballesteros-Cánovas
373 et al., 2015). Therefore, our results are supporting the previously stated drawbacks of flood
374 hazard assessments based on short-flow gauge series, as they tend to underreport extreme events
375 (Baker, 2008).

376 Rather than focusing at the catchment scale, this paper has illustrated how tree-ring
377 reconstructions can be used to inform managers dealing with regional flood frequency analyses
378 in poorly gauged, but highly vulnerable regions such as the IHR. The methodology used in this
379 study in fact overcomes the usual limitations related to the spatial distribution of trees (or any
380 other paleoflood proxy) suitable for reconstruction and its comparability with systematic rain-
381 gauge records located elsewhere in the system. We are convinced that the approach presented

382 here has major methodological advantages over more conventional work, since the
383 reconstruction of past floods can indeed be realized at the most suitable river reaches (i.e. stable
384 bedrock, existence of evidence, and critical flow conditions; Ballesteros-Canovas et al., 2015;
385 Ballesteros Cánovas et al., 2011; Benito, 2004; Bodoque et al., 2015; Jarrett and England, 2002)
386 for which uncertainties in paleoflood reconstructions can be minimized. As these conditions can
387 only rarely be found at the location of the gauge station, direct flow comparison has so far been
388 limited due to the increase/decrease of catchment area between the sites. Here, we overcome this
389 limitation by showing that ungauged floods reconstructed with tree-ring records in the headwater
390 catchment, and consequently at some distance of the gauge station, indeed are a very useful and
391 valuable proxy for flood-frequency analyses.

392 This approach is especially interesting in the geographical context of the IHR (Kullu district is
393 part of this region), where the inaccessibility and/or lack of highly-accurate topographic data
394 generally hampers the reconstruction of flood magnitude data in appropriate river reaches.
395 Therefore, field-based surveys and sampling used to be extremely difficult here, due to the very
396 high stream power of the surveyed catchments which limited the use of two dimensional models
397 or the critical-depth method to minimize uncertainties related to the calibration of roughness
398 parameter. These constraints resulted in only a handful of suitable river reaches for which an
399 adequate estimation and representation of channel cross-sections was possible. Remaining
400 uncertainties can indeed be addressed with a Bayesian approach as used in this study so as to
401 consider the ungauged flood extreme as a range of values provided by the resolution of
402 Manning's equation and by varying the roughness parameter by $\pm 25\%$ with respect to the initial
403 set of values. Yet, we are well aware that the estimation of peak flow may represent a source of
404 uncertainties (i.e. up to 30%) due to the initial hydraulic assumption (i.e. uniform flow) related to

405 Manning's equation (Jarret and England, 2002). Nevertheless, the values obtained are very
406 reasonable and still present the only viable solution to overcome the notorious lack of data in
407 poorly gauged IHR valleys. Therefore, this study has shown quite clearly that the coupled
408 paleoflood-regional flood frequency approach indeed opens a large set of possibilities for a more
409 useful integration of past flood reconstructions into systematic records over large homogeneous
410 regions. In fact, the information provided by the regional flood frequency allows an upscaling of
411 hydrological information to conduct regional flood hazard assessments, and can thus contribute
412 to the design and successful implementation of adaptation policies to reduce adverse impacts of
413 climate change in the IHR region.

414 **6 Conclusions**

415 Tree-ring based flood reconstructions have been successfully applied in the Indian Himalayan
416 region (IHR), demonstrating their potential for flood hazard analyses. We have also illustrated
417 the value of a coupled paleoflood record (derived from tree-ring series) with flood regional
418 frequency approaches and have shown that the coupling of the two datasets enables
419 maximization of the gathered information, improvement of peak discharge estimates for specific
420 return periods and a reduction of uncertainties. Besides the fact that we provide the first flood
421 frequency estimation for the region, the second key factor for flood risk evolution is the built
422 environment and the ever increasing population density in the floodplains of the IHR, which will
423 in fact have an impact on losses during future flood situations. In view of the significantly
424 increased (and ever increasing) exposure level of populations and their goods in floodplains
425 (Gardner, 2002; Gardner et al., 2002), future flood disasters must be expected in the IHR region.
426 Our flood reconstruction supplements the lack of long-term data and therefore can improve the

427 basic knowledge on flood processes, as demanded in Disaster Management Plans. As such this
428 study can contribute to the adaption to climate change in the region.

429 **Acknowledgments**

430 Hydrological data has been obtained from Bhakra Beas Management Board (BBMB) and
431 Irrigation and Public Health Department, Himachal Pradesh. The authors acknowledge the
432 financial support from the Indian Himalayas Climate Adaptation Programme (IHCAP;
433 www.ihcap.in) of the Swiss Agency for Development and Cooperation (SDC). The authors thank
434 Dr. Victor Baker, Dr. Matthew Therrell as well as two anonymous reviewers for their insight
435 comments during the revision process.

436 **References**

- 437 Allen, S.K., Rastner, P., Arora, M., Huggel, C., Stoffel, M., 2015. Lake outburst and debris flow
438 disaster at Kedarnath, June 2013: hydrometeorological triggering and topographic
439 predisposition. *Landslides*. doi:10.1007/s10346-015-0584-3
- 440 Arbella, E., Stoffel, M., Bollschweiler, M., 2010. Wood anatomical analysis of *Alnus incana*
441 and *Betula pendula* injured by a debris-flow event. *Tree Physiol.* 30, 1290–1298.
- 442 Arbella, E., Corona, C., Stoffel, M., Fonti, P., Decaulne, A., 2012a. Defining an adequate
443 sample of earlywood vessels for retrospective injury detection in diffuse-porous species.
444 *PLoS one* 7: e38824.
- 445 Arbella, E., Fonti, P., Stoffel, M., 2012b. Duration and extension of anatomical changes in
446 wood structure after cambial injury. *J. Exp. Bot.* 63, 3271-3277.

- 447 Attri, S.D., Tyagi, A., 2010. Climate profile of India. *Environ. Meteorol. India Meteorol. Dep.* 1–
448 122. doi:10.1007/s12524-010-0015-9
- 449 Baker, V. R., 2008. Paleoflood hydrology: Origin, progress, prospects. *Geomorphology*, 101(1),
450 1-13.
- 451 Ballesteros, J.A., Stoffel, M., Bollschweiler, M., Bodoque, J.M., Díez-Herrero, A., 2010a. Flash-
452 flood impacts cause changes in wood anatomy of *Alnus glutinosa*, *Fraxinus angustifolia* and
453 *Quercus pyrenaica*. *Tree Physiol.* 30, 773–781. doi:10.1093/treephys/tpq031
- 454 Ballesteros, J. A., Stoffel, M., Bodoque, J.M., Bollschweiler, M., Hitz, O., Díez-Herrero, A.,
455 2010b. Changes in Wood Anatomy in Tree Rings of *Pinus pinaster* Ait. Following
456 Wounding by Flash Floods. *Tree-Ring Res.* 66, 93–103. doi:10.3959/2009-4.1
- 457 Ballesteros Cánovas, J.A., Eguibar, M., Bodoque, J.M., Díez-Herrero, A., Stoffel, M., Gutiérrez-
458 Pérez, I., 2011. Estimating flash flood discharge in an ungauged mountain catchment with
459 2D hydraulic models and dendrogeomorphic palaeostage indicators. *Hydrol. Process.* 25,
460 970–979. doi:10.1002/hyp.7888
- 461 Ballesteros, J.A., Bodoque, J.M., Díez-Herrero, A., Sanchez-Silva, M., Stoffel, M., 2011b.
462 Calibration of floodplain roughness and estimation of flood discharge based on tree-ring
463 evidence and hydraulic modelling. *J. Hydrol.* 403, 103–115.
464 doi:10.1016/j.jhydrol.2011.03.045
- 465 Ballesteros-Cánovas, J.A., Sanchez-Silva, M., Bodoque, J.M., Díez-Herrero, A., 2013. An
466 Integrated Approach to Flood Risk Management: A Case Study of Navaluenga (Central
467 Spain). *Water Resour. Manag.* 27, 3051–3069. doi:10.1007/s11269-013-0332-1

- 468 Ballesteros-Cánovas, J.A., Rodríguez-Morata, C., Garófano-Gómez, V., Rubiales, J.M.,
469 Sánchez-Salguero, R., Stoffel, M., 2014. Unravelling past flash flood activity in a forested
470 mountain catchment of the Spanish Central System. *J. Hydrol.* 529, 468–479.
471 doi:10.1016/j.jhydrol.2014.11.027
- 472 Ballesteros-Canovas, J.A., Stoffel, M., St George, S., Hirschboeck, K., 2015a. A review of flood
473 records from tree rings. *Prog. Phys. Geogr.* 39, 794–816. doi:10.1177/0309133315608758
- 474 Ballesteros-Cánovas, J.A., Czajka, B., Janecka, K., Lempa, M., Kaczka, R.J., Stoffel, M., 2015b.
475 Flash floods in the Tatra Mountain streams: Frequency and triggers. *Sci. Total Environ.*
476 511, 639–648. doi:10.1016/j.scitotenv.2014.12.081
- 477 Ballesteros-Cánovas, J.A., Stoffel, M., Spyt, B., Janecka, K., Kaczka, R.J., Lempa, M., 2015c.
478 Paleoflood discharge reconstruction in Tatra Mountain streams. *Geomorphology* 4–13.
479 doi:10.1016/j.geomorph.2015.12.004
- 480 Ballesteros-cánovas, J.A., Tasaduq, H.K., Shabir, H.A., Shah, B., 2016. Documenting historic
481 and recent extreme floods in Kashmir 18, 11990.
- 482 Benito, G., and V.R.Thorndycraft., 2004. Systematic, Palaeoflood and Historical Data for the
483 Improvement of Flood Risk Estimation, Methodological Guidelines.
- 484 Benito, G., Sopeña, A., Sánchez-Moya, Y., Machado, M.J., Pérez-González, A., 2003.
485 Palaeoflood record of the Tagus River (Central Spain) during the Late Pleistocene and
486 Holocene. *Quat. Sci. Rev.* 22, 1737–1756. doi:10.1016/S0277-3791(03)00133-1
- 487 Bodoque, J.M., Díez-Herrero, A., Eguibar, M.A., Benito, G., Ruiz-Villanueva, V., Ballesteros-

- 488 Cánovas, J.A., 2015. Challenges in paleoflood hydrology applied to risk analysis in
489 mountainous watersheds - A review. *J. Hydrol.* 529, 449–467.
490 doi:10.1016/j.jhydrol.2014.12.004
- 491 Cell, D.M., n.d. Government of Himachal Pradesh.
- 492 Chase, T.N., Knaff, J.A., Pielke, S.A., Kalnay, E., 2003. Changes in global monsoon circulations
493 since 1950. *Nat. Hazards* 29, 229–254. doi:10.1023/A:1023638030885
- 494 Chow, V.T., 1964. *Handbook of applied hydrology*.
- 495 Corriell, F., 2002. Reconstruction of a paleoflood chronology for the middlebury river gorge
496 using tree scars as flood stage indicators. Middlebury College.
- 497 Duan, K., Yao, T., Thompson, L.G., 2006. Response of monsoon precipitation in the Himalayas
498 to global warming. *J. Geophys. Res. Atmos.* 111, 1–8. doi:10.1029/2006JD007084
- 499 Gaál, L., Szolgay, J., Kohnová, S., Hlavčová, K., Viglione, A., 2010. Inclusion of historical
500 information in flood frequency analysis using a Bayesian MCMC technique: a case study
501 for the power dam Orlick, Czech Republic. *Contrib. to Geophys. Geod.* 40, 121–147.
502 doi:10.2478/v10126-010-0005-5
- 503 Gardner, J.S., 2002. Natural Hazards Risk in the Kullu District, Himachal Pradesh, India*.
504 *Geogr. Rev.* 92, 282–306. doi:10.1111/j.1931-0846.2002.tb00008.x
- 505 Gardner, J.S., Saczuk, E., 2004. Systems for hazards identification in high mountain areas: An
506 example from the Kullu District, western Himalaya. *J. Mt. Sci.* 1, 115–127.
507 doi:10.1007/BF02919334

- 508 Gaume, E., Gaál, L., Viglione, A., Szolgay, J., Kohnová, S., Blöschl, G., 2010. Bayesian MCMC
509 approach to regional flood frequency analyses involving extraordinary flood events at
510 ungauged sites. *J. Hydrol.* 394, 101–117. doi:10.1016/j.jhydrol.2010.01.008
- 511 George, B. and St George., 2015. Flooding, Structural Flood Control Measures, and Recent
512 Geomorphic Research along the Red River, Manitoba, Canada, in: Springer (Ed.),
513 Geomorphic Approaches to Integrated Floodplain Management of Lowland Fluvial Systems
514 in North America and Europe. New York, pp. 87–117.
- 515 Germain, D., Filion, L., Héту, B., 2009. Snow avalanche regime and climatic conditions in the
516 Chic-Choc Range, eastern Canada. *Clim. Change* 92, 141–167. doi:10.1007/s10584-008-
517 9439-4
- 518 Goswami, B.N., Xavier, P.K., 2005. ENSO control on the south Asian monsoon through the
519 length of the rainy season. *Geophys. Res. Lett.* 32, 1–4. doi:10.1029/2005GL023216
- 520 Hirabayashi, Y., Mahendran, R., Koirala, S., Konoshima, L., Yamazaki, D., Watanabe, S., Kim,
521 H., Kanae, S., 2013. Global flood risk under climate change. *Nat. Clim. Chang.* 3, 816–821.
522 doi:10.1038/nclimate1911
- 523 Hobbey, D.E.J., Sinclair, H.D., Mudd, S.M., 2012. Reconstruction of a major storm event from
524 its geomorphic signature: The Ladakh floods, 6 August 2010. *Geology* 40, 483–486.
525 doi:10.1130/G32935.1
- 526 Hosking, J.R.M., Wallis, J.R., 1987. Parameter and Quantile Estimation for the Generalized
527 Pareto Distribution. *Technometrics* 29, 339–349. doi:10.1198/016214507000000932

- 528 Jarrett, R.D., and J.England., 2002. Reliability of paleostage indicators for paleoflood studies, in:
529 Ancient Floods, Modern Hazards: Principles and Applications of Paleoflood Hydrology.
530 Water Science and Application, Vol. 5. pp. 91–109.
- 531 Kjeldsen, T.R., Macdonald, N., Lang, M., Mediero, L., Albuquerque, T., Bogdanowicz, E.,
532 Bra'zdil, R., Castellarin, A., David, V., Fleig, A., Gu'l, G.O., Kriauciuniene, J., Kohnova',
533 S., Merz, B., Nicholson, O., Roald, L.A., Salinas, J.L., Sarauskiene, D., S'raj, M.,
534 Strupczewski, W., Szolgay, J., Toumazis, A., Vanneuville, W., Veijalainen, N., Wilson, D.,
535 2014. Documentary evidence of past floods in Europe and their utility in flood frequency
536 estimation. *J. Hydrol.* 517, 963–973. doi:10.1016/j.jhydrol.2014.06.038
- 537 Kogelnig-Mayer, B., Stoffel, M., Schneuwly-Bollschweiler, M., Hübl, J., Rudolf-Miklau, F.,
538 2011. Possibilities and Limitations of Dendrogeomorphic Time-Series Reconstructions on
539 Sites Influenced by Debris Flows and Frequent Snow Avalanche Activity. *Arctic, Antarct.*
540 *Alp. Res.* 43, 649–658. doi:10.1657/1938-4246-43.4.649
- 541 Kripalani, R.H., Kulkarni, A., 1997. Rainfall variability over South–east Asia—connections with
542 Indian monsoon and ENSO extremes: new perspectives. *Int. J. Climatol.* 17, 1155–1168.
543 doi:10.1002/(SICI)1097-0088(199709)17:11<1155::AID-JOC188>3.0.CO;2-B
- 544 Kumar, K., Hoerling, M., Rajagopalan, B., 2005. Advancing dynamical prediction of Indian
545 monsoon rainfall. *Geophys. Res. Lett.* 32, 1–4. doi:10.1029/2004GL021979
- 546 Mathison, C., Wiltshire, A., Dimri, A.P., Falloon, P., Jacob, D., Kumar, P., Moors, E., Ridley, J.,
547 Siderius, C., Stoffel, M., Yasunari, T., 2013. Regional projections of North Indian climate
548 for adaptation studies. *Sci. Total Environ.* 468–469. doi:10.1016/j.scitotenv.2012.04.066

- 549 McCord, V.A., 1990. Augmenting Flood Frequency Estimates using Flood-Scarred Trees.
550 University of Arizona.
- 551 National Disaster Management Policy, 2009, 2009. National Policy on Disaster Management
552 2009 . Government of India.
- 553 O'Connell, D.R.H., 2005. Nonparametric Bayesian flood frequency estimation. *J. Hydrol.* 313,
554 79–96. doi:10.1016/j.jhydrol.2005.02.005
- 555 O'Connor, J.E., Ely, L.L., Wohl, E.E., Stevens, L.E., Melis, T.S., Kale, V.S., Baker, V.R., 1994.
556 A 4500-Year Record of Large Floods on the Colorado River in the Grand Canyon, Arizona.
557 *J. Geol.* 102, 1–9. doi:10.1086/629644
- 558 Parthasarathy, B., Sontakke, N.A., Monot, A.A., Kothawale, D.R., 1987. Droughts/floods in the
559 summer monsoon season over different meteorological subdivisions of India for the period
560 1871–1984. *J. Climatol.* 7, 57–70. doi:10.1002/joc.3370070106
- 561 Rajeevan, M., Gadgil, S., Bhate, J., 2008. Active and Break Spells of the Indian Summer
562 Monsoon. NCC Research Report: March 2008.
- 563 Ranatunge, E., Malmgren, B.A., Hayashi, Y., Mikami, T., Morishima, W., Yokozawa, M.,
564 Nishimori, M., 2003. Changes in the Southwest Monsoon mean daily rainfall intensity in
565 Sri Lanka: Relationship to the El Niño-Southern Oscillation. *Palaeogeogr. Palaeoclimatol.*
566 *Palaeoecol.* 197, 1–14. doi:10.1016/S0031-0182(03)00383-3
- 567 Rodriguez-Morata, C., Ballesteros-Cánovas, J.A., Trappmann, D., Beniston, M., Stoffel, M.,
568 2016. Regional reconstruction of flash flood history in the Guadarrama range (Central

- 569 System, Spain). *Sci. Total Environ.* 550, 406–417. doi:10.1016/j.scitotenv.2016.01.074
- 570 Ruiz-Villanueva, V., Allen, S., Arora, M., Goel, N.K., Stoffel, M., 2016. Recent catastrophic
571 landslide lake outburst floods in the Himalayan mountain range. *Prog. Phys. Geogr.*
572 doi:10.1177/0309133316658614
- 573 Ruiz-Villanueva, V., Díez-Herrero, A., Bodoque, J.M., Ballesteros Cánovas, J.A., Stoffel, M.,
574 2013. Characterisation of flash floods in small ungauged mountain basins of Central Spain
575 using an integrated approach. *Catena* 110, 32–43. doi:10.1016/j.catena.2013.06.015
- 576 Sah, M.P., Mazari, R.K., 2007. An overview of the geoenvironmental status of the Kullu Valley,
577 Himachal Pradesh, India. *J. Mt. Sci.* 4, 003–023. doi:10.1007/s11629-007-0003-x
- 578 Sah, M.P., Mazari, R.K., 1998. Anthropogenically accelerated mass movement, Kulu Valley,
579 Himachal Pradesh, India. *Geomorphology* 26, 123–138. doi:10.1016/S0169-
580 555X(98)00054-3
- 581 Schneuwly, D.M., Stoffel, M., Dorren, L.K.A., Berger, F., 2009. Three-dimensional analysis of
582 the anatomical growth response of European conifers to mechanical disturbance. *Tree*
583 *Physiol.* 29, 1247–1257. doi:10.1093/treephys/tpp056
- 584 Shroder, J.F., 1978. Dendrogeomorphological analysis of mass movement on Table Cliffs
585 Plateau, Utah. *Quat. Res.* 9, 168–185. doi:10.1016/0033-5894(78)90065-0
- 586 Šilhán, K., 2015. Frequency, predisposition, and triggers of floods in flysch Carpathians:
587 Regional study using dendrogeomorphic methods. *Geomorphology* 234, 243–253.
588 doi:10.1016/j.geomorph.2014.12.041

- 589 St. George, S., 2010. Tree rings as paleoflood and paleostage indicators., in: M. Stoffel;
590 M.Bollschweiler; D.R. Butler; and B.H. L. (Ed.), Tree-Rings and Natural Hazards. Tree-
591 Rings and Natural Hazards. A State-of-the-Art. Springer Dordrecht Heidelberg, London,
592 New York, pp. 233–239.
- 593 St. George, S., Nielsen, E., 2003. Palaeoflood records for the Red River, Manitoba, Canada,
594 derived from anatomical tree-ring signatures. *The Holocene* 13, 547–555.
595 doi:10.1191/0959683603hl645rp
- 596 Stedinger, J.R., 2001. Framework With Partial Duration and Annual Maximum Series 37, 2559–
597 2567.
- 598 Stoffel, M., 2008. Dating past geomorphic processes with tangential rows of traumatic resin
599 ducts. *Dendrochronologia* 26, 53–60. doi:10.1016/j.dendro.2007.06.002
- 600 Stoffel, M., Corona, C., 2014. Dendroecological Dating of Geomorphic Disturbance in Trees.
601 *Tree-Ring Res.* 70, 3–20. doi:10.3959/1536-1098-70.1.3
- 602 Stoffel, M., Perret, S., 2006. Reconstructing past rockfall activity with tree rings: Some
603 methodological considerations. *Dendrochronologia* 24, 1–15.
604 doi:10.1016/j.dendro.2006.04.001
- 605 Stoffel, M., Wilford, D.J., 2012. Hydrogeomorphic processes and vegetation: Disturbance,
606 process histories, dependencies and interactions. *Earth Surf. Process. Landforms* 37, 9–22.
607 doi:10.1002/esp.2163
- 608 Stoffel M, Bollschweiler M, Butler DR, et al. 2010. Tree rings and natural hazards: a state-of-art.

- 609 Berlin, New York: Springer
- 610 Terray, P., Dominiak, S., 2005. Indian ocean sea surface temperature and El Niño-southern
611 oscillation: A new perspective. *J. Clim.* 18, 1351–1368. doi:10.1175/JCLI3338.1
- 612 Therrell, M.D., Bialecki, M.B., 2015. A multi-century tree-ring record of spring flooding on the
613 Mississippi River. *J. Hydrol.* 529, 490–498. doi:10.1016/j.jhydrol.2014.11.005
- 614 Turner, A., 2013. *The Indian Monsoon in a Changing Climate.*
- 615 UN, 2005. *Hyogo Framework for Action 2005-2015. Strategy 1–25.*
616 doi:10.1017/CBO9781107415324.004
- 617 Viglione, A., 2014. nsRFA: Non-supervised Regional Frequency Analysis. R Packag. version
618 0.7-12.
- 619 Yanosky, T. M., and R.D., J., 2002. Dendrochronologic evidence for the frequency and
620 magnitude of paleofloods, in: *Ancient Floods, Modern Hazards.* pp. 77–89.
- 621 Yim, S.Y., Wang, B., Liu, J., Wu, Z., 2014. A comparison of regional monsoon variability using
622 monsoon indices. *Clim. Dyn.* 43, 1423–1437. doi:10.1007/s00382-013-1956-9
- 623 Zielonka, T., Holeksa, J., Ciapała, S., 2008. A reconstruction of flood events using scarred trees
624 in the Tatra Mountains, Poland. *Dendrochronologia* 26, 173–183.
625 doi:10.1016/j.dendro.2008.06.003

626

627 **Captions**

628 **Figure 1.** Study sites at Kullu district, Himachal Pradesh (Indian Himalayan Region).

629 **Figure 2.** Examples of scars used as paleostage indicators (PSI) of past floods. These trees are
630 growing in the floodplain of a tributary stream (A) and in the main channel (B) of the Thiertan
631 River in the valley of the same name. For details see Figure 1.

632 **Figure 3.** Temporal occurrence of floods at Kullu district as a combination of dated floods at
633 each of the catchments studied (black vertical lines), and years with flow measurement values
634 exceeding the 90th percentile of gauge station records (grey vertical lines).

635 **Figure 4.** Composite flood occurrence at Kullu district based on tree-ring and flow gauge station
636 records. Sample depth indicates the decreasing number of trees with scars available for analysis
637 as one goes back in time.

638 **Figure 5.** Example of the regional (upper panel) and site-specific (lower panel) flood frequency
639 assessment for Thiertan, Sainj, and Beas Rivers. The inclusion of tree-ring records provides an
640 improved estimate of discharge values for specific return periods and reduces uncertainty in
641 discharge estimates for events with large return periods.

642 **Table 1.** Flood events per catchment, including those dated with tree rings (years given in bold)
 643 and those with extreme runoff recorded in the flow series (the word “extreme” here refers to the
 644 exceedance of the 90th percentile of runoff values).

645

N° of catchments	Flood years
1	1910, 1919 , 1967, 1968, 1971 , 1972, 1973, 1974 , 1975, 1981 , 1994, 2002, 2009, 2013, 2014
2	1989, 1992, 1997 , 1999, 2001, 2003, 2006 , 2008, 2012
3	1978, 1988, 1995, 2011
4	1993, 2005, 2010

646

647 **Table 2:** Reconstructed peak discharge for past flood events at Kullu district

Site	Catchment		Year	T_{100} (m^3/s)	Limit		
	area (in km^2)	STDEV (m^3/s)			low (m^3/s)	Limit _{upp} (m^3/s)	
Sainj river	470		2005	719	185	533	904
Sainj river	470		2009	191	49	142	240
Sainj river	470		2003	494	127	366	621
Sainj river	470		2006	639	164	474	804
Sainj river	470		1997	244	88	155	333
Sainj river	470		2011	181	46	135	227
Sainj river	470		1978	655	169	486	824
Thiertan river	112		2005	1869	482	1387	2351

648

649

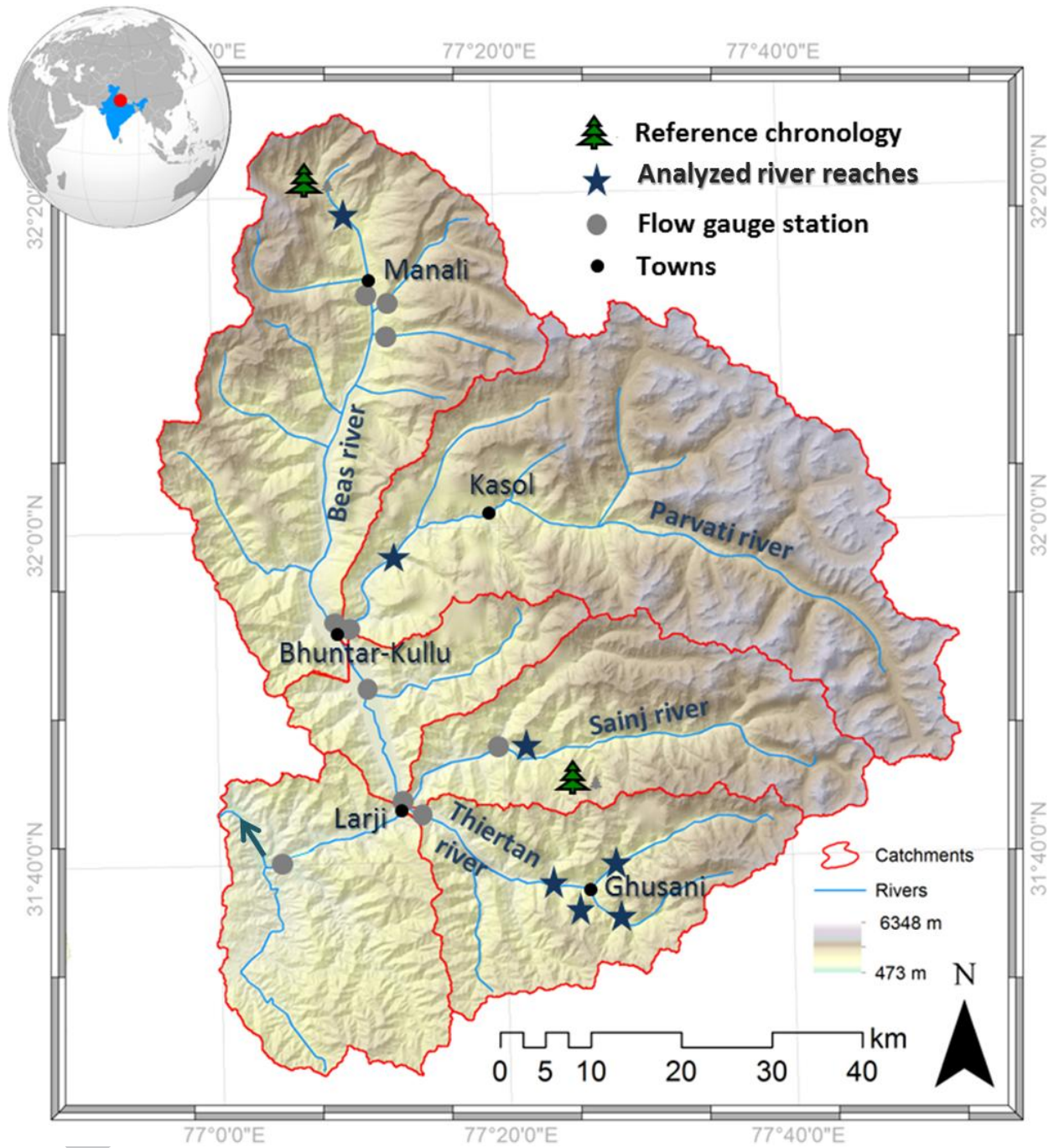
650

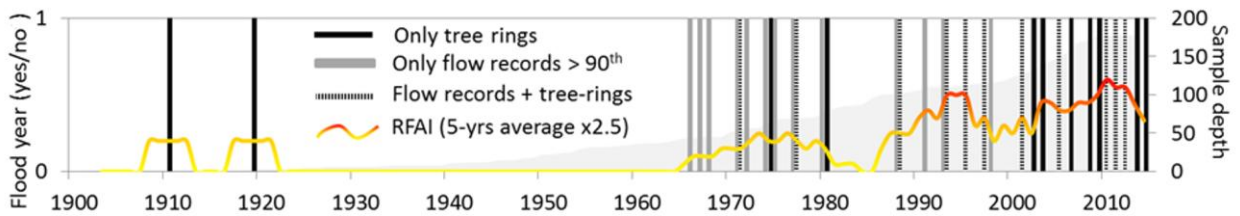
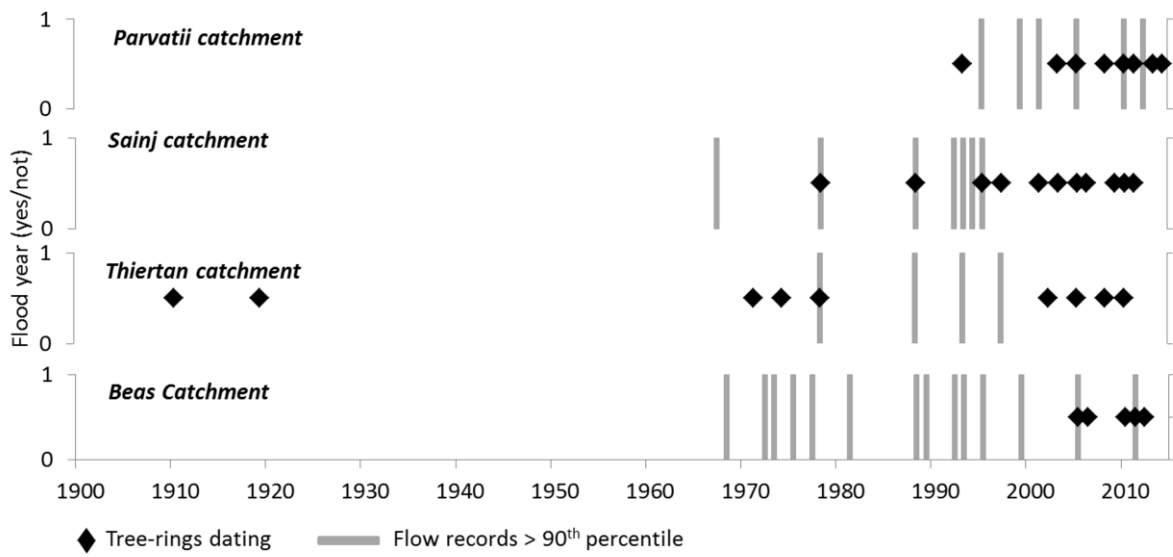
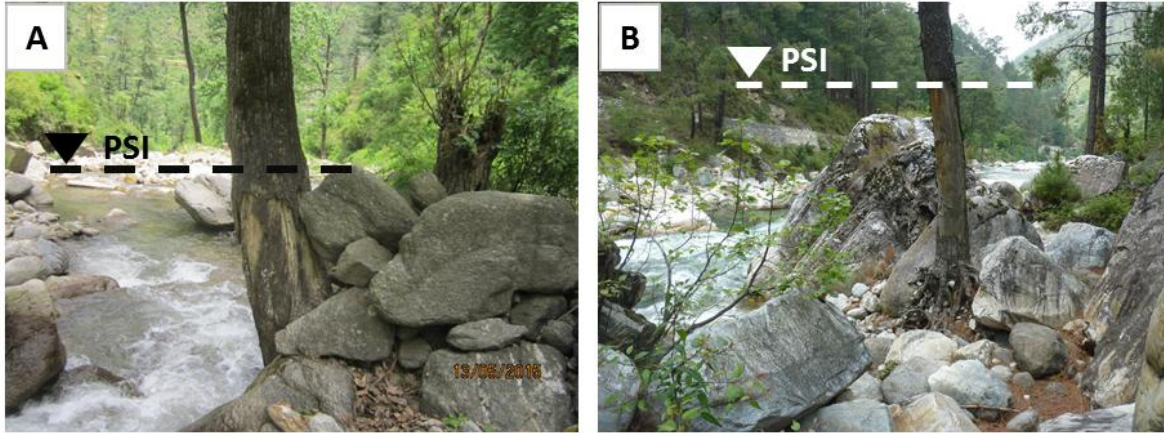
651

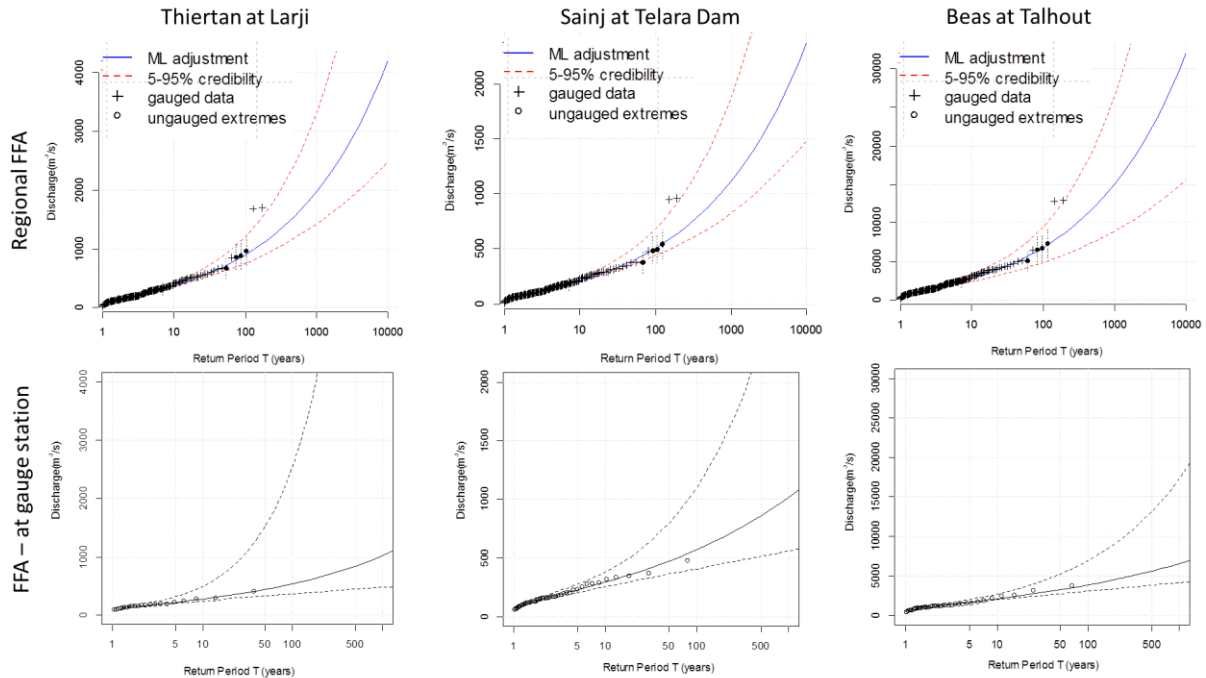
652

Table 3: Comparison of the 100-year flood and uncertainties between the regional flood frequency (tree-ring and gauge station data) and the flood frequency at each gauge station.

Flow gauge station/site	Area (km ²)	Reconstructed regional flood frequency (m ³ /s)		Flood frequency at gauge station (m ³ /s)				
		T100	Δ 90IC	T100		Δ 90IC		
				T100	Δ 90IC	Δ T100	Δ 90IC	
Thiertan at Larji	658	909	500	1182	4636	77	11	
Sainj at Larji	920	1250	625	500	581	250	108	
Sainj at Telara Dam	647	889	480	516	2116	172	23	
Baragam Nallah	22	44	22	47	110	94	20	
Allain Nallah	176	280	133	107	213	263	63	
Hurla Nallah	232	379	172	121	466	314	37	
Beas Bhuntar	3826	4545	3182	2500	2500	182	127	
Beas Manali	349	500	250	565	739	88	34	
Beas Pandho	6264	7692	4615	6154	6538	125	71	
Beas Talhout	5788	7143	3929	3667	4000	195	98	
						Average	176	59
						STDEV	81	40







Highlights:

- The implementation of Disaster Risk reduction strategies is hampered by the lack of data in the Indian Himalaya region
- Tree ring based paleoflood reconstruction complement the limited existing flow gauge records
- The inclusion of extreme unrecorded flood events in upper catchments improve the regional flood frequency assessment